

Morphing Quadcopters: A Comparison Between Proposed and Prominent Foldable Quadcopters

Thanat Tothong
Computer Engineering
California State University,
Fullerton
Fullerton, USA
thanat.t@csu.fullerton.edu

James Samawi
Computer Engineering
California State University,
Fullerton
Fullerton, USA
jsamawi@csu.fullerton.edu

Ameya Govalkar
Computer Engineering
California State University,
Fullerton
Fullerton, USA
ameya.govalkar@csu.fullerton.edu

Kiran George
Computer Engineering
California State University,
Fullerton
Fullerton, USA
kgeorge@fullerton.edu

Abstract—Quadcopters are entering numerous fields of work and require unique functionality for each area that they are deployed. They are also becoming more adaptable to terrain and changes in the environment. For example, a quadcopter that can fold could be used by Search and Rescue teams who need to navigate tight and inaccessible spaces. This paper presents a notable insight into two variants of morphing drones that have been assembled with keeping different morphing modes and mechanisms in mind. The first proposed quadcopter uses servo motors on each propeller arm to achieve a folding motion mid-flight, while the second proposed quadcopter uses a novel method of utilizing micro linear actuators to reduce its size in all directions. Flight data for the proposed quadcopters will be presented, along with comparing total weight, flight time, size reduction, and other parameters with similar morphing quadcopters from the research community.

Keywords—Drone, Morphing Quadcopter, Pixhawk, aerial, morphology.

I. INTRODUCTION

A. Overview

To adapt to certain terrains or scenarios, it may be beneficial for drones to change their shape to optimize speed and mobility. This feature is called morphing and can be applied particularly well with drones. Morphology, with respect to drones, refers to the general shape the drone takes on while stationary or midflight. In some cases, the user can switch to the desired morphology before or during flight by toggling a button.

A morphing quadcopter can quickly become very complex easily. With many moving parts it may not be the most optimal over time. The *Transformable Multirotor* [1] is a 2-D transforming aerial vehicle. This large drone uses six independent, multilink rotor arms to transform midflight while also enabling the user to “whole-body grasp” different types of objects. Morphologies this particular drone takes on are the cylinder and the convex polygon modes [1]. The convex polygon is unique in that the rotor arms adjust its internal folding angle with respect to the object being picked up. A year later, the same team of researchers created the *DRAGON* aerial robot [2]. This aerial robot uses four independently linked dual-rotor arms to move freely in 3-D space. Unlike its predecessor, the goal of the *DRAGON* is to be able to adapt to the terrain by freely and autonomously changing shape midflight to squeeze into tight and inaccessible spaces [2]. These two large aerial vehicles are complex and are far from user friendly. By keeping the morphing mechanisms and range of motion simple, it will

preserve the purpose of the drone and do the job without requiring any complex folding mechanisms [3].



Fig. 1. Proposed servo-based morphing quadcopter during a test flight.

Therefore, the inspiration for the proposed quadcopter designs were found from two previous quadcopters called *The Foldable Drone* [3] and the *ElbowQuad* [4]. Another notable morphing drone is the *Agile Robotic Fliers*, which is a simulated quadcopter that uses a combination of a servo motors and elastic bands to reel in its propellers to mimic how birds bring in their wings to navigate narrow apertures [5]. And lastly, the recent morphing quadcopter called the *Passively Morphing Quadcopter* uses a spring assisted servo motor to drastically fold the four propellers in a downward fashion in order to greatly reduce the size of the drone [6]. Although impossible to navigate the drone in its folded state, it was tested to clear gaps that are 38 cm² in size while the drone itself is 54 cm² in size [6].

This paper will compare two morphing quadcopters: one prototype version with a servo-based design (rotor arms that fold) and another iteration with an actuator-based design (rotor arms that retract). The proposed servo-based and actuator-based designs will be compared to all the previously mentioned drone designs. Following this introduction will be a background behind the mathematical models of the proposed morphing drones. This paper will then break down the first and second quadcopter designs, starting with the first servo-based design implementation. Following that is the section about the gathered data for roll, pitch, and yaw for each morphology. After that comes the section about comparing the specifications of the proposed quadcopters and the referenced drones, including flight times, weights, size ratios, and other data points. Finally, this paper is closed with concluding thoughts and acknowledgments.

B. Background

The two drone designs, servo-based and actuator-based, each have flight/morph mode variations of their own, and each flight mode suits a specific task. The prototype of the first quadcopter design utilizes four programmed servos, which perform the morphing mid-flight with two folding morphologies and a default morphology for efficiency. By independently turning the programmed servos underneath each propeller arm, many different shapes are created along the X-Y plane. The chosen morphologies for the servo-based drone are the “O” and “H” formations, excluding the default “X” formation in the neutral position. This iteration of the quadcopter will be referred to as the “servo-based quadcopter” in this paper. The second version of the quadcopter utilizes actuators. This iteration will be referred to as the “actuator-based quadcopter” in this paper. The actuator-based iteration of the drone uses four programmed micro linear actuators that perform a single morphology by retracting the blades inward to reduce its size along the X-Y plane, hence enabling it to fit into tighter spaces.

In Fig. 2, the top-down view of a mathematical model of a drone shows the starting angle (θ) location of each propeller arm (propellers are labeled 1, 2, 3, and 4), which will help describe each morphology moving forward. Each arm angle from θ_1 (front left), θ_2 (back left), θ_3 (back right), and θ_4 (front right) are adjusted to form a specific morphology.

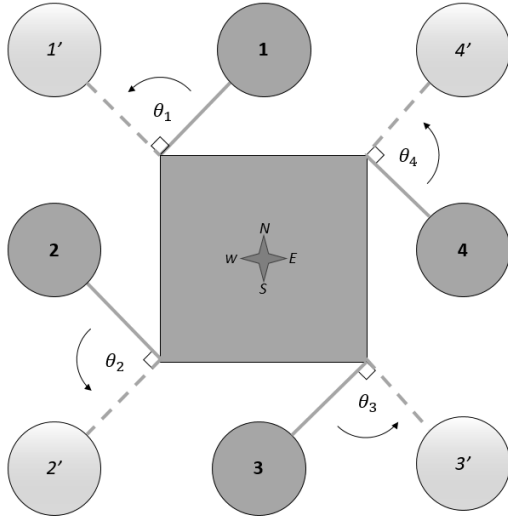


Fig. 2. Mathematical drone model detailing arm angles on the X-Y plane.

Following this mathematical model of a drone, let each independent servo arm angle θ start at zero (assuming the shape of an O). The default position of the servo-based drone is the X formation (Fig. 2) and is achieved by turning each arm by $\theta_i = \pi/2$, $i = 1, 2, 3, 4$. To fly through narrow gaps, the drone can utilize the H formation (Fig. 3a, $\theta_1 = \theta_3 = \pi/4$, $\theta_2 = \theta_4 = 3\pi/4$). By folding all the arms to the center of the body, there will be a significant size reduction and will assume the O formation (Fig. 3b and Fig. 2, $\theta_i = 0$, $i = 1, 2, 3, 4$).

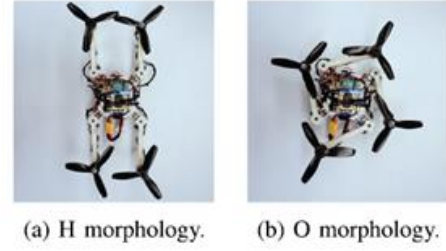


Fig. 3. Morphologies that the proposed servo-based quadcopter utilizes [3].

It should be noted that the flight mode for the micro linear actuator-based drone design utilizes the actuators beneath the propellers to retract inwards or expand outwards by command. This morphology takes advantage of the standard position of the drone with the neutral “X” position (Fig. 6). The neutral X morphology trades off task-specific morphologies for improved mobility [3] and, in general, shrinks the diameter of the drone by the length of the linear actuator shaft on each propeller by roughly 45mm.

The Center of Mass (CoM) was calculated with respect to the individually powered servos or actuators from the four drone arms ranging from $\theta_1 \dots \theta_4$. This is contrary to the standard method of finding CoM by using the geometric center of the drone or calculating an offset of the whole system [3]. The offset vector (1) for the servo-based drone and the offset vector (2) for the actuator-based drone can be calculated in 3-D space using the equations provided:

$$\text{Let } \vec{r}_{CoM,servo} \in \mathbb{R}^3 \text{ such that } \vec{r}_{CoM,servo} = \frac{m_{frame}\vec{r}_{frame} + \sum_{i=1}^4(m_{arm}\vec{r}_{arm,i} + m_{motor}\vec{r}_{motor,i} + m_{rotor}\vec{r}_{rotor,i})}{m_{frame} + \sum_{i=1}^4(m_{arm,i} + m_{motor,i} + m_{rotor,i})} \quad (1)$$

$$\begin{aligned} \text{Let } \vec{r}_{CoM,actuator} \in \mathbb{R}^3 \text{ such that } \vec{r}_{CoM,actuator} = & \frac{m_{frame}\vec{r}_{frame} + \sum_{i=1}^4(m_{arm}\vec{r}_{arm,i} + m_{motor}\vec{r}_{motor,i} + m_{rotor}\vec{r}_{rotor,i})}{m_{frame} + \sum_{i=1}^4(m_{arm,i} + m_{shaft,i} + m_{motor,i} + m_{rotor,i})} \\ & + \frac{\sum_{i=1}^4 m_{shaft,i} \vec{r}_{shaft,i}}{m_{frame} + \sum_{i=1}^4(m_{arm,i} + m_{shaft,i} + m_{motor,i} + m_{rotor,i})} \end{aligned} \quad (2)$$

Again, the CoM equation must be adjusted for the independently turning arms, even though it appears to be folding or expanding synchronously. The mass and distance vector for any 3-D printed part, motor, and rotor located on the arms of their respective drone is ultimately summed, and the calculation resumes from there. Also note that for the actuator-based drone (2), the arm is the actuator itself but excluding the shaft, which is another moving mass. Also, it is worth noting for the previous drone (1) that the servos are stationary and are attached to the frame of the drone, so they can be considered a part of the structure. Finding the CoM of these drones can be beneficial for future implementation using simulations, so that one can find the CoM of current or new designs, or if one must displace weight to achieve a well-balanced vehicle.

C. Motivation

The authors seek designs that exceed the limited movement of drones when traversing narrow gaps—inspired by birds that cruise forests with their dynamic wings. This morphing drone was designed to achieve a similar movement, including optimized performance such as flight time, agility, and user-friendliness. This paper strays away from the static-frame quadcopter norm and prototype dynamic designs that were thought to be capable of accomplishing a morph during flight with good performance, user-friendly controls, and multiple useful flight modes which can be activated on-the-go.

II. IMPLEMENTATION

A. Design One: Servo Design



Fig. 4. Proposed servo-based morphing quadcopter.

1) Mechanical system:

All of the parts of the frame were 3-D printed to provide rapid prototyping, consistency, and simplicity for modification. The structure consists of four parts, which are a top framework, bottom framework, arms, and supports. Each piece was designed to ensure that it was strong enough to hold torque from the servos, to be light for providing maximum flight time, and less use of materials. The morphing mechanism was implemented by installing four servos at the tips on the base. Servo horns and arms are attached for generating the movement. To counter torque from the propellers, supports are installed between the bottom frame and arms assisting torqued load for servos.

2) Electronic system:

The design firstly was built around the size of a racing drone, 250 - 300 mm, after considering prices and availability. The first component is a flight controller; for this project, Pixhawk4 was selected because of high reliability, and it has an open-source software for modifications. Pixhawk4 transmits signals towards the 33A 2~5S electronic speed controllers (ESCs). The EMAX 2306-2400kv motors are used for this design due to its compatibility, because the size of said drone requires high KV motors to operate. To control the shapes of the drones, pilots can toggle a three-way switch on the RC remote control. The signal from the receiver is forwarded into an Arduino Pro Mini 328 and then makes a decision for the position of servos.

The power system of this drone consists of two parts. A power management board will be supplied by a 12v, 3-cell battery that draws the voltage and current to the electronic speed controllers, then the ESCs will drive those motors (ref on how ESC works). The power management board also has two regulators that convert 12v into 5v for supplying the pixhawk4 and includes a backup system. Another power system goes to a 5v regulator, which feeds an Arduino Pro Mini and four servos. To supply the system, a 2200 mAh 3-cell battery was chosen. The supply was divided into two parts, which are the direct voltage from a battery that goes to a power management board that supplies the motors, Pixhawk, and voltage regulator. This, in return, supplies a morphing system that includes the Arduino Pro Mini and servos.

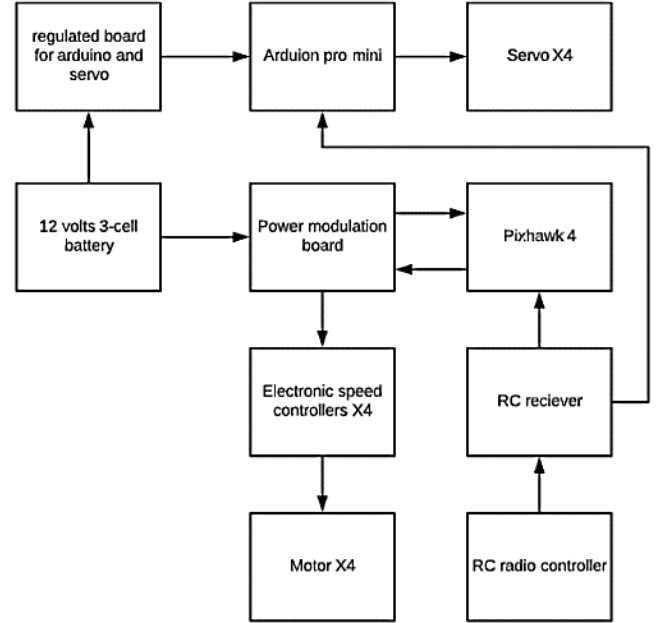


Fig. 5. Servo-based morphing quadcopter design visualization.

B. Design Two: Actuator Design

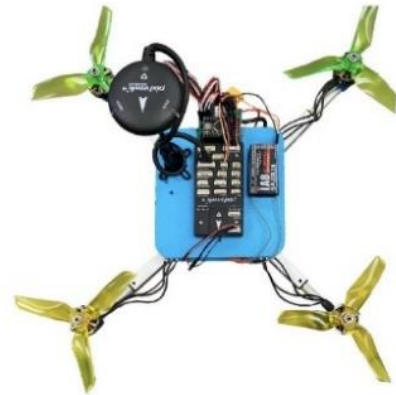


Fig. 6. Proposed actuator-based morphing quadcopter.

1) Mechanical system:

Instead of using servos for changing shapes of a drone, this design uses actuators for morphing. Four micro linear actuators

are placed underneath the bottom part of the drone. At the tip of each actuator will be attached to a motor. Like the servo design, all pieces in this design were 3-D printed for quality and consistency purposes. The model of actuators is the L16-R Miniature Linear Servos from Actuatorix. The reason behind this choice was that the actuators were compatible with Arduino, which made the interfacing easier.

2) Electronic system:

To compare the performance between the two designs, the components that are utilized are the same, including the flight controller, motors, ESCs, the power management module, and propellers. The circuit that controls servos is still the same as well, but the code for the control system in the Arduino needed to be reprogrammed. Like the servo design, the two-way switch is used to control the actuators.

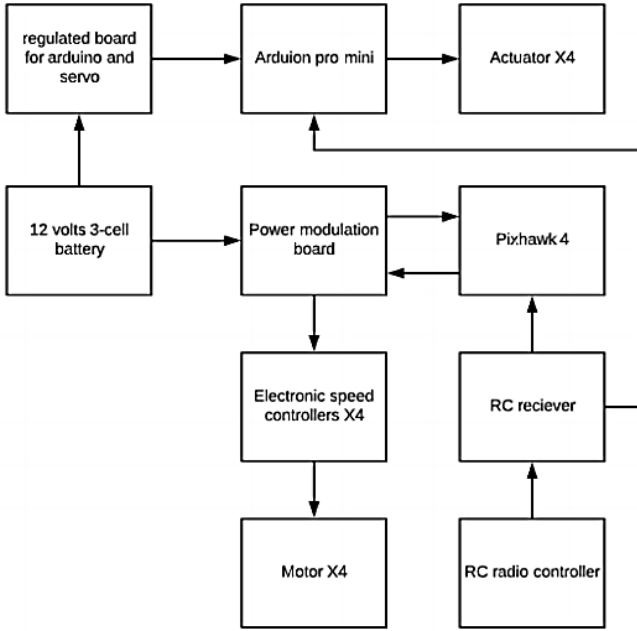


Fig. 7. Actuator-based morphing quadcopter design visualization.

III. DATA AND COMPARISON

The flight information gathered from the flight logs of both the servo-based and the actuator-based quadcopters is used to evaluate their respective flight capabilities and efficiencies. Then selected specifications are then compared to the referenced foldable drones. The data presented below was obtained from test flight logs for both servo-based and actuator-based drones. The ArduPilot logs were first recorded and then converted to MATLAB readable format, primarily to facilitate the processing of logs under the MATLAB environment.

Plotted data was compared to the flight roll, pitch, and yaw with destination roll, pitch, and yaw, respectively, for each of the proposed drones and their morphologies. This comparison was made by overlapping the flight and destination values over the same revolution vs. time plot. The scatter plots are graphical comparisons that help in verifying the visual stability of the drone during test flights with plotted real-time log data (Fig. 9-23). It also helps in locating the points of instability during the

flight, such as changes in thrust vectoring from a change in morphology or environmental factors like wind direction.

A. Quadcopter Altitude Modeling

The combined angular velocity of four rotors which are directly connected to the propellers result in vertical thrust which drives the quadcopter altitude as a single body. Characteristically, rotor propellers placed in opposed position will rotate in the same directions and side-by-side ones will rotate oppositely. Controlling the angular velocity of the four rotors will consequently result in a dynamic movement with force and moment transmission which lead to lift, pitch, roll or yaw rotations moment inertia [7]. Fig. 8. Illustrates these rotations and are explained as follows: rotation around X-axis as roll movement, rotation around Y-axis as pitch movement, and rotation around Z-axis as yaw movement.

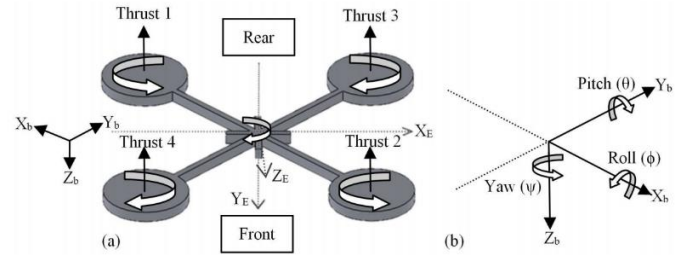


Fig. 8. Quadcopter schematic: (a) The structure of a quadcopter (b) Illustration of Roll, Pitch and Yaw [6].

B. Roll vs. Destination Roll Scatter Plots

In Fig. 9 through Fig. 13. compared are the test-flight roll and the destination roll — which is the ideal values for the flight from point A to B, using scatter plots with their respective values for each of the three modes of the servo-based quadcopter (Fig. 9, 10 and 11) and the two modes of the actuator-based quadcopter (Fig. 12 and 13). The more linear these plots are, or close together the points are, the more stable the drone is with changes in mid-flight morphology or environmental factors.

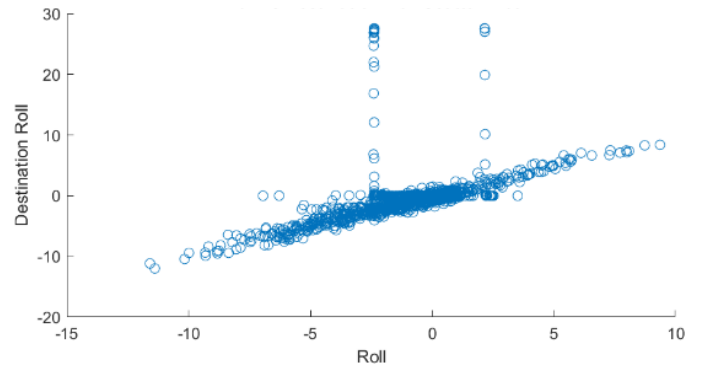


Fig. 9. Servo-based H mode.

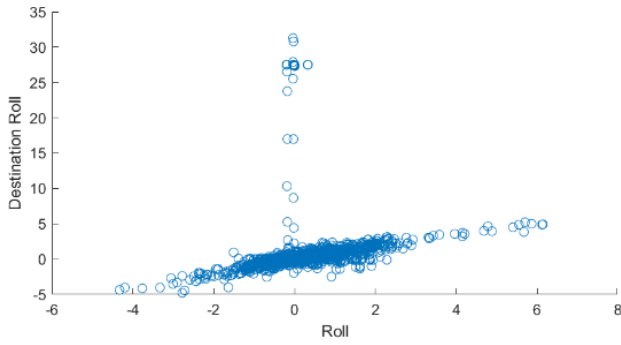


Fig. 10. Servo-based O mode.

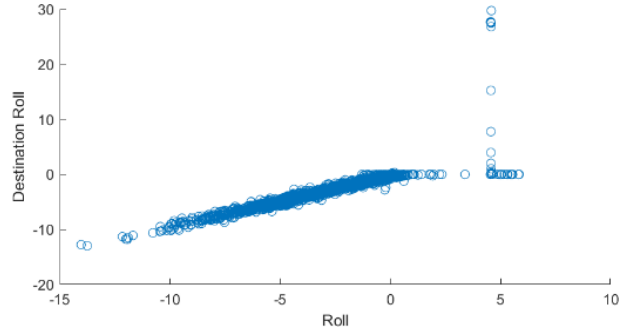


Fig. 11. Servo-based X mode.

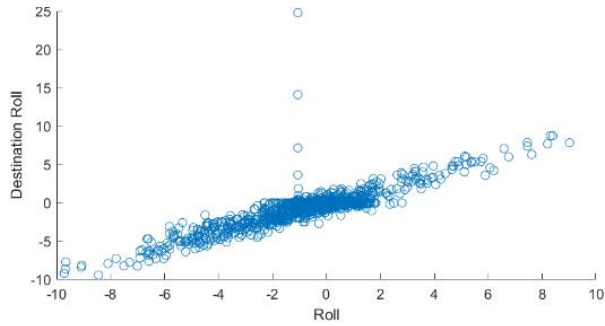


Fig. 12. Actuator-based Extend mode.

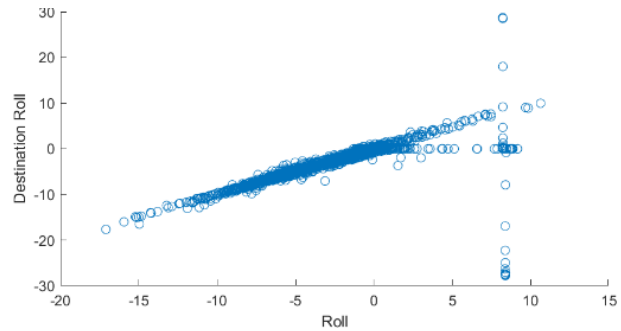


Fig. 13. Actuator-based Retract mode.

C. Pitch vs. Destination Pitch Scatter Plots

In Fig. 14 through Fig. 18, compared are the test-flight pitch and the destination pitch — which is the ideal values for the flight from point A to B, using scatter plots with their respective values for each of the three modes of the servo-based

quadcopter (Fig. 14, 15 and 16) and the two modes of the actuator-based quadcopter (Fig. 17 and 18). The more linear these plots are, or close together the points are, the more stable the drone is with changes in mid-flight morphology or environmental factors.

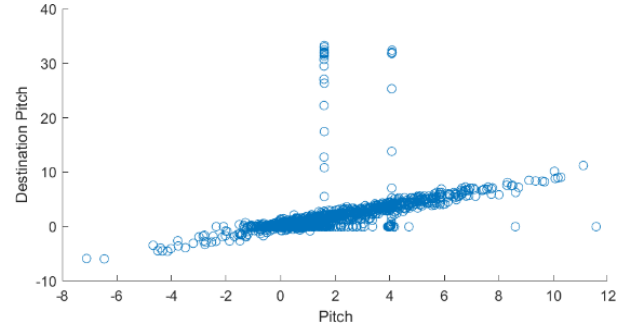


Fig. 14. Servo-based H mode.

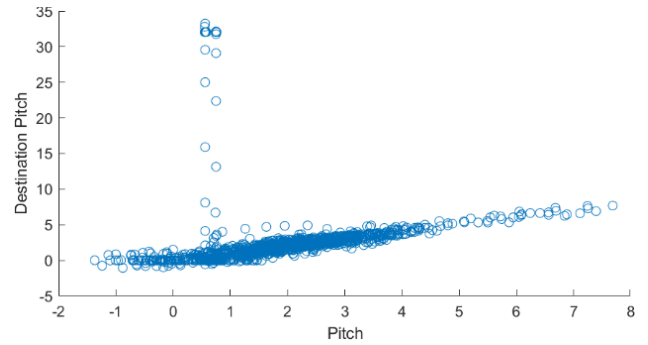


Fig. 15. Servo-based O mode.

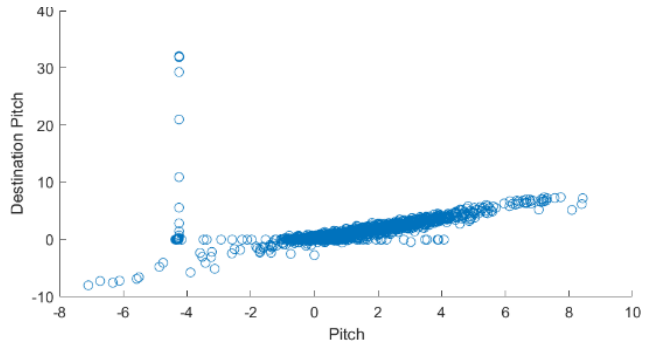


Fig. 16. Servo-based X mode.

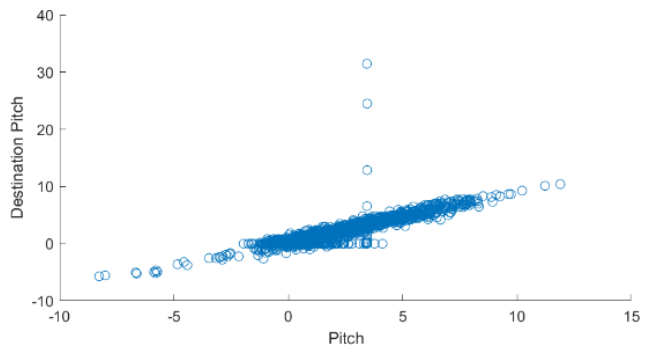


Fig. 17. Actuator-based Extend mode.

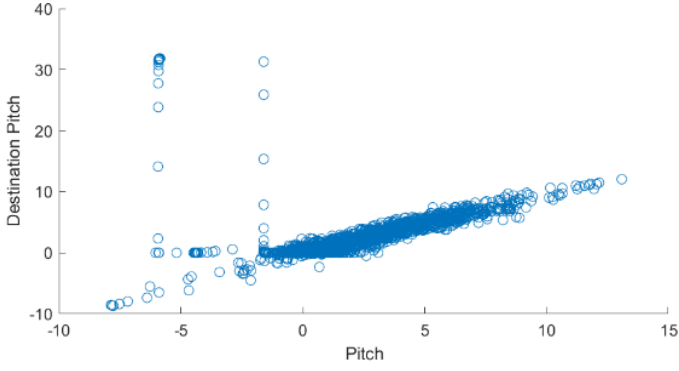


Fig. 18. Actuator-based Retract mode.

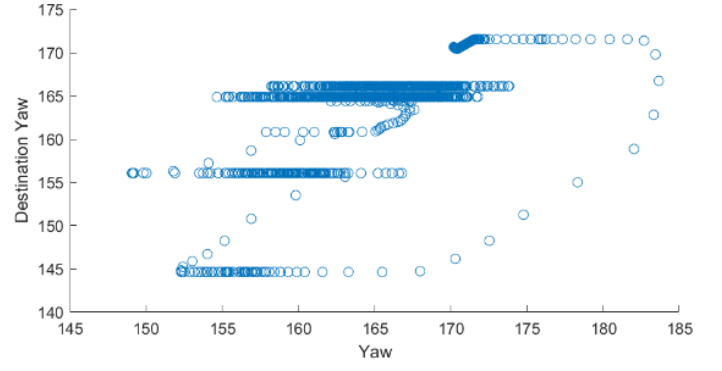


Fig. 21. Actuator-based Extend mode.

D. Yaw vs. Destination Yaw Scatter Plots

In Fig. 19 through Fig. 23, compared are the test-flight yaw and the destination yaw — which is the ideal values for the flight from point A to B, using scatter plots with their respective values for each of the three modes of the servo-based quadcopter (Fig. 19, 20 and 21) and the two modes of the actuator-based quadcopter (Fig. 22 and 23). Since these plots contain points which are distant from one another and not linear (and discontinuity), they suggest instability with the designs of both the servo-based and actuator-based quadcopter yaw direction.

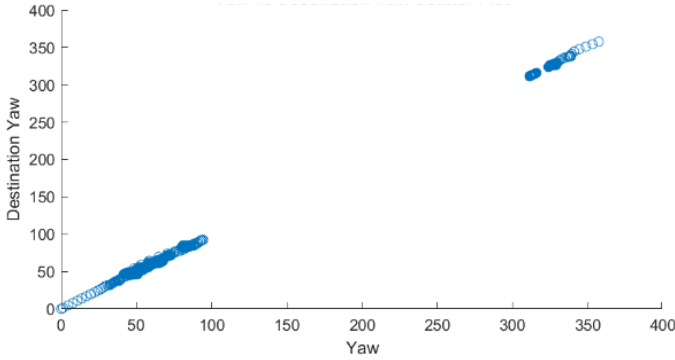


Fig. 19. Servo-based O mode.

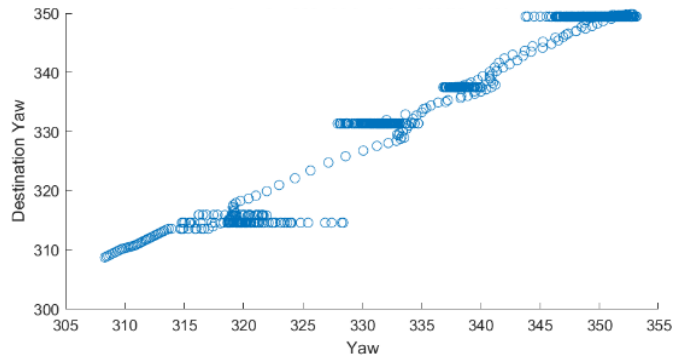


Fig. 20. Servo-based X mode.

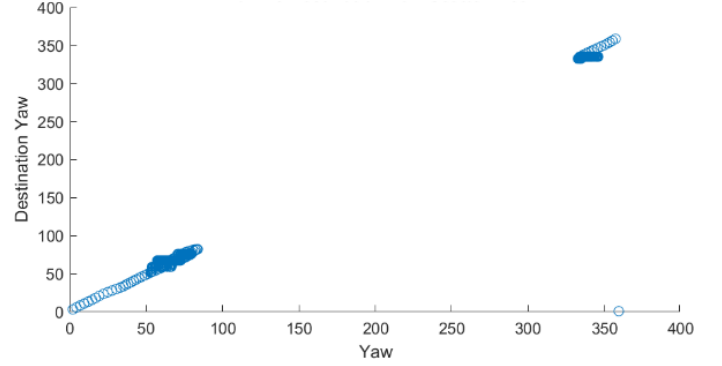


Fig. 22. Actuator-based Retract mode.

D. Specifications

The specifications from both servo-based and actuator-based quadcopters are compared to the referenced drones in TABLE I. Some parameters are labeled as “N/A” because those values are not given in their respective referenced papers. The *Transformable Multirotor* [1] and *DRAGON* [2] aerial vehicles have extremely complex morphologies, and with their large size, it is challenging to make fair comparisons with miniature quadcopters.

Compared to the *Foldable Drone* [3], the proposed quadcopters, servo-based and actuator-based, seem to be noticeably heavier. This is due to the mechanisms in both drones, the larger 3-D printed frames, and the battery of choice for both the drones. The 3-cell 25C discharge 2200 mAh LiPo battery aided the two proposed quadcopters in their added weights (by 185 g) and their increase in flight times compared to *The Foldable Drone*. The servo-based proposed quadcopter did an excellent job with size reduction, as well as significantly increasing the flight time of the O morphology by 261.7%. The Actuator-based quadcopter (and the only actuator-based quadcopter in this table) struggled with its total weight, even with its light frame, due to the weight of the four micro linear actuators. Another consequence was the reduced flight time, although the actuators did help with the size reduction in the retract morphology, which closely mimics the O morphology, compared to the servo-based quadcopter and *The Foldable Drone*.

In TABLE I., notice the values obtained in the “Size by Ratio” row is normalized by the selected drone’s default

morphology values. For example, the default morphology for the *Agile Robotic Fliers* [5] is the un-folded mode, so those ratios are set to (1,1). Based on that particular drone's folded mode parameters p_i , the size ratio using the un-folded mode parameters p_x is given by p_i/p_x [3]. The smallest y-axis size ratio belongs to the *Agile Robotic Fliers* (0.48), allowing it to fly through very narrow apertures. A consequence of this size imbalance comes with "instability in the folded position" in their simulated design [5]. The *Passively Morphing Quadcopter* achieves an astounding size reduction of around 48% along the x and y axes [6]. The size reduction of the actuator-based quadcopter is about 11% (from 36 cm² to 32 cm²) for the sake of comparison. A drawback of this mid-flight morph is that it is only temporary and cannot sustain this morphology longer than roughly 0.59 seconds [6]. Lastly, the *ElbowQuad* [4] had the most morphologies out of all seven drones (5), although there was no information regarding the sizes of the *ElbowQuad* nor its weight and flight times.

Out of the two proposed quadcopters, the servo-based morphing quadcopter has the most desirable parameters listed below. The efficient, simplistic (not complex) design of the

servo-based quadcopter achieves the feature of folding midflight without instability in the roll and pitch directions. Unlike the *Agile Robotic Fliers* and the *Passively Morphing Quadcopter* with their band/spring servo motor morphing mechanism, the servo-based morphing quadcopter and *The Foldable Drone* are medium sized quadcopters which have desired, simplistic mechanisms with less moving parts. Among these two drones, the servo-based drone dominates in flight time and sizing between X, O, and H modes. Parameters aside, the servo-based quadcopter was assembled with ease, and the same schematic was shown to work with the actuator-based quadcopter, which has the same layout as the servo-based drone except the servo motors were replaced with micro linear actuators.

The plans for the quadcopters moving forward are to work on the mentioned stability issues for both drones, and then move onto the next stage of research and implementation. The next stage is the implementation of Brain-Computer Interface (BCI) with the current Arduino Pro Mini to achieve hands-free, midflight morphing.

TABLE I. COMPARING PARAMETERS FOR PROPOSED QUADCOPTERS TO THE FIVE REFERENCED FOLDABLE DRONES

	Proposed Quadcopters					The Foldable Drone [3]				Elbowquad [4]	Agile Robotic Fliers [5]		Passively Morphing Quadcopter [6]	
Folding Mechanism	Actuator-based		Servo-based			Servo-based				Servo-based	Servo-based with band assistance		Servo-based with spring assistance	
Total Weight (g)	905		835			580				N/A	N/A		940	
Number of Modes	2		3			4				5	2		2	
Morphology Names	Extend	Retract	H	X	O	H	X	O	T	Std., Std. Transl., Stable Hover, Angled Hover, Transl. Flat	Un-folded	Folded	Un-folded	Folded
Size (x, y) (cm)	36, 36	32, 32	29, 45	36, 36	33, 33	N/A	N/A	N/A	N/A	25, 25	40.8, 26.8	56, 12.8	54, 54	28, 28
Size by Ratio	1, 1	0.88, 0.88	0.81, 1.25	1, 1	0.91, 0.91	0.9, 1.59	1, 1	1.19, 1.19	1.1, 0.85	N/A	1,1	1.37, 0.48	1, 1	0.52, 0.52
Flight Time (s)	167	160	209	350	340	210	253	94	195	N/A	N/A	N/A	N/A	N/A
Flight Time by Ratio	1	0.96	0.60	1	0.97	0.83	1	0.37	0.77	N/A	N/A	N/A	N/A	N/A

Proposed Servo-based and Actuator-based Quadcopters Ratio Comparison Chart

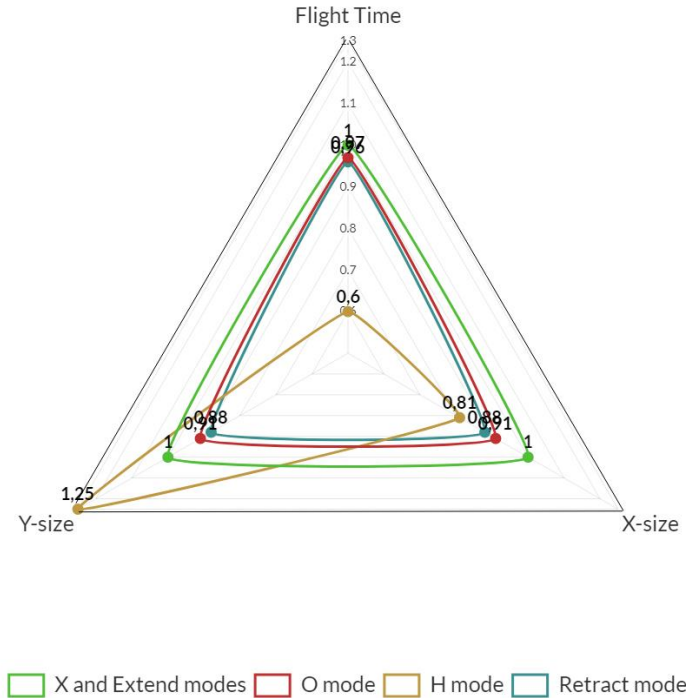


Fig. 23. The radar chart represents selected parameters from TABLE I. as ratios for flight time, x-axis and y-axis sizes for morphologies pertaining to the proposed servo-based and actuator-based morphing quadcopters. The green data points are normalized values for the neutral states of both quadcopters.

IV. CONCLUSION

The paper presented went over the design and process of creating the servo-based and actuator-based iterations of the morphing quadcopter while also showing flight data and side-by-side analysis of certain aspects for the proposed quadcopter and several other quadcopters. Through testing each morphology for both the proposed quadcopters, it proves to be useful in certain scenarios like fitting in tight spaces. Its relatively simple design implementation made it easy to iterate the design from servo-based to actuator-based. In the end, the first iteration of the quadcopter that uses servo motors for mid-flight morphing turned out to be a more reliable, all-around quadcopter compared to the second iteration of the proposed quadcopter and the several referenced works.

RELATED WORK

The drone morphing capabilities are innovative and beneficial but can tend to be slow due to human reaction times in a fast-paced environment. Integrating drone morphing with a brain-computer interface (BCI) is a relatively new concept and a significant improvement on how drones can be controlled by its users.

ACKNOWLEDGMENT

The authors would like to thank the open-source Pixhawk community for their helpful online presence and the University of California State Fullerton for providing this quadcopter research opportunity.

REFERENCES

- [1] M. Zhao, K. Kawasaki, X. Chen, S. Noda, K. Okada and M. Inaba, "Whole-body aerial manipulation by transformable multirotor with two-dimensional multilinks," in *Proc. IEEE Int. Conf. Robot. Automat.*, Jun. 2017, pp. 5175-5182.
- [2] M. Zhao, T. Anzai, F. Shi, X. Chen, K. Okada and M. Inaba, "Design, Modeling, and Control of an Aerial Robot DRAGON: A Dual-Rotor-Embedded Multilink Robot With the Ability of Multi-Degree-of-Freedom Aerial Transformation," in *IEEE Robotics and Automation Letters*, vol. 3, no. 2, April 2018.
- [3] D. Falanga, K. Kleber, S. Mintchev, D. Floreano, and D. Scaramuzza "The Foldable Drone: A Morphing Quadrotor That Can Squeeze and Fly," *IEEE Robotics and Automation Letters*, vol. 4, pp. 209-211, 2019.
- [4] T. Devlin, R. Dickerhoff, K. Durney, A. Forrest, P. Pansodtee, A. Adabi, and M. Teodorescu, "Elbowquad: Thrust vectoring quadcopter," in *Proc. AIAA Inf. Syst.-AIAA Infotech Aerosp.*, 2018, p. 0893.
- [5] V. Riviere, A. Manecy, and S. Viollet, "Agile Robotic Fliers: A Morphing-Based Approach," *2018 Soft Robotics*, vol. 5, no. 5, pp. 541-553.
- [6] N. Bucki and M. W. Mueller, "Design and Control of a Passively Morphing Quadcopter," *2019 International Conference on Robotics and Automation (ICRA)*, Montreal, QC, Canada, 2019, pp. 9116-9122.
- [7] Kuantama, Endrowednes & Vesselenyi, Tiberiu & Dzitac, S. & Tarca, Radu. (2017). "PID and Fuzzy-PID control model for quadcopter attitude with disturbance parameter," *International Journal of Computers Communications & Control*, 2012, p. 519-532.